PREMIER COLLOQUE IMAGE
Traitement, Synthèse, Technologie et Applications
BIARRITZ — Mai 1984 —

RECONSTRUCTION CONIQUE : HAUTE RESOLUTION SANS REARRANGEMENT

FAN-BEAM RECONSTRUCTION : HIGH RESOLUTION WITHOUT REARRANGEMENT

S.C. TAN, D. LE GALL, T.H. NGUYEN
M. GAMEIRO PAIS, C. BENCHIMOL

THOMSON-CGR : 48 rue Camille Desmoulins 92130 ISSY-LES-MOULINEAUX

RESUME

En Tomodensitométrie, il est bien connu que l'acquisition sur un tour complet, avec un détecteur centré, présente une redondance. Il est aussi connu qu'en décentrant le détecteur d'une fraction de pas d'échantillonnage, les données acquises sur un tour complet ne sont plus redondantes et peuvent être réarrangées, puis interpolées pour accroître l'échantillonnage spatial. Après quoi, il suffit d'appliquer une reconstruction adaptée pour obtenir un gain en résolution spatiale. Cette approche du mode haute résolution, par réarrangement des données, présente cependant des inconvénients. En effet, les techniques de réarrangement demandent beaucoup de temps, à moins d'utiliser des matériels spécialisés. En plus, elles sont très sensibles aux imprécisions de la machine (décentrage non parfait, échantillonnage vue) et au mouvement du patient.

Nous proposons dans ce papier, une nouvelle approche du mode Haute Résolution qui présente l'intérêt de ne recourir à aucune technique de réarrangement. En géométrie parallèle, la théorie proposée est parfaitement exacte. En géométrie conique, bien que la transposition ne soit pas mathématiquement exacte, le gain en résolution spatiale est cependant substantiel. La performance de la méthode proposée a été démontrée, en géométrie conique, dans les conditions d'une acquisition réelle des données.

Mots clés : Tomodensitométrie, détecteur décentré, Haute Résolution, sans réarrangement, Reconstruction conique, Tomographie à Rayons X.

SUMMARY

In CAT, it is known that with a centered detector, data collection over 360° presents a redundancy. It is also known that by off-setting the detector by a fraction of ray sampling, data collected over 360° are no longer redundant and can be rearranged and interpolated to increase the spatial sampling. Subsequently, an appropriate reconstruction needs only to be applied to increase the spatial resolution. However, this approach to high resolution presents some drawbacks. First, the procedure of rearrangement is time consuming unless specialized hardware is used. Furthermore, inaccuracies in data measurement, due to detector drift or patient motion, can produce various artifacts.

In this paper, we present a new approach to High Resolution, in which no rearrangement scheme is required. In Parallel geometry, the proposed theory is perfectly exact. In Fan Beam geometry, although the transposition is not mathematically exact, the gain of resolution is nevertheless substantial. The effectiveness of the proposed method has been demonstrated, in Fan Beam geometry, under conditions of real data acquisition.

Key words : CAT, off-set, High Resolution, without rearrangement, Fan-Beam Reconstruction, X-Ray Tomography.

S.C. TAN, D. LE GALL, T.H. NGUYEN
M. GAMEIRO PAIS, C. BENCHIMOL

RECONSTRUCTION CONIQUE : HAUTE RESOLUTION SANS REARRANGEMENT

FAN-BEAM RECONSTRUCTION : HIGH RESOLUTION WITHOUT REARRANGEMENT

I. Introduction

In CT Reconstruction, the ray sampling is known to be a significant factor of the spatial resolution |1,2|. On 3rd generation Scanners (Rotate-Rotate without translationnal movement, cf. fig 1) the spatial sampling frequency of each projection is fixed once for all when designing the detector ; the latter can be characterized by its ray sampling period ΔY.

Therefore, in order to increase the spatial resolution of these machines, several authors have studied some possibilities to artificially increase the ray sampling frequency. Since the data acquisition over 360° with a centered detector presents a redundancy, Peters and Lewitt |3| suggested the acquisition over 360° with a quarter ray detector offset ($\Delta Y/4$) (cf. fig 1). The data collected in this manner are no longer redundant and can be rearranged, then interpolated to form new projections with a higher sampling rate. In |3|, the rearranged data correspond to a set of projections obtained with an equivalent parallel geometry. This procedure requires two-step interpolation :
- Interpolation between views
- Interpolation between rays

Other possibilities of data rearrangement are found in |4| ; in particular the existence of rearrangement scheme without interpolation is shown. These techniques present however some drawbacks :
1) Storage problems (In order to form one new projection, it is necessary to simultaneously process many original views)
2) Data processing time
3) Lack of Robustness (high sensitivity to mechanical inaccuracies, patient motion...)

In this paper, a new approach to high resolution is proposed in which no rearrangement is required. The proposed method consists in performing independently on each original projection of N measurements a simple operation (to be detailed later) which produces 2N measurements. Afterwards an appropriate Filtered-Backprojection algorithm |5| needs to be applied to obtain an increase in spatial resolution.

Part II deals with the theoretical development in Parallel geometry. Part III concerns the application to Fan Beam geometry. Finally Part IV presents the conclusions.

II. Theory in Parallel Geometry

A. Preliminary studies

We shall study, in this chapter, some properties of the Filtered-Backprojection associated with a symmetric kernel k (k(s)=k(-s)). Let's introduce :

(1) the Deconvolution D defined by :

$\forall f$ function of 2 variables (θ,s),
if $g = D.f$ then :

$$g(\theta,s) \triangleq \int_{-\infty}^{+\infty} f(\theta,t)k(s-t)dt$$

(2) the Backprojection R defined by :

$$(Rg)(x,y) \triangleq \begin{cases} \int_0^{2\pi} g(\theta, x\cos\theta + y\sin\theta)d\theta & (2.1) \\ \quad \text{(acquisition over 360°)} & \\ \int_0^{\pi} g(\theta, x\cos\theta + y\sin\theta)d\theta & (2.2) \\ \quad \text{(acquisition over 180°)} & \end{cases}$$

$\mathcal{L}_{2\pi}$ and $\mathcal{L}_{\pi}$ are defined by the following relations:

$\mathcal{L}_{2\pi} f \triangleq$ (2.1) $\quad \mathcal{L}_{\pi} f \triangleq$ (2.2)

Remarkable properties of $\mathcal{L}_{2\pi}$ and $\mathcal{L}_{\pi}$ are (see |6| for proof) :

P.1- $\mathcal{L}_{2\pi}$ and $\mathcal{L}_{\pi}$ are linear operators

P.2- If we defined $\bar{f}$ by $\bar{f}(\theta,s) \triangleq f(\theta+\pi,-s)$, then we obtain :
$\mathcal{L}_{2\pi} f = \mathcal{L}_{\pi} f + \mathcal{L}_{\pi} \bar{f} = \mathcal{L}_{\pi} (f+\bar{f})$

P.3- If $f(\theta,s) = p_\theta(s)$ the linear attenuation function, then $\bar{f}=f$ and $\mathcal{L}_{2\pi} f = 2\,\mathcal{L}_{\pi} f$

Discretization

Without loss of generality and for simplicity, we consider only the discretization of s while leaving θ continuous (*). We will represent the discretization of an operator or function by a superscript N. Let's introduce the following relations :

$s_i \triangleq ih + \frac{h}{2}$ (3) and $s'_i \triangleq i.h$ (3') ;

(3) ==> $-s_i = s_{-(i+1)}$ (4) and

(3') ==> $-s'_i = s'_{-i}$ (4') ;

$\nu_c = \frac{1}{2h}$ the Nyquist frequency associated with the spatial sampling period h ; (5)

$f^N(\theta,i) \triangleq f(\theta,s_i)$ (6)

$g^N(\theta,i) \triangleq g(\theta,s_i)$ (7)

$k^N(i) \triangleq k(s'_i)$ (kernel sampled at points $s'_i = i.h$) (8)

(9) hypothesis : In the following, we assume $f(\theta,.)$ and k to be band-limited to $[-\nu_c, \nu_c]$.
It follows that $g = Df$ is also band-limited to $[-\nu_c, \nu_c]$.

(10) Discrete deconvolution D^N (associated with the kernel k^N)

$$D^N f^N(\theta,i) \triangleq \sum_j f^N(\theta,j)\, k^N(i-j)$$

(9) ==> $g^N = D^N.f^N$

(*) The only condition to be satisfied is for $\pi/\Delta\theta$ to be an integer, where $\Delta\theta$ is the angular sampling distance.

S.C. TAN, D. LE GALL, T.H. NGUYEN
M. GAMEIRO PAIS, C. BENCHIMOL

RECONSTRUCTION CONIQUE : HAUTE RESOLUTION SANS REARRANGEMENT

FAN-BEAM RECONSTRUCTION : HIGH RESOLUTION WITHOUT REARRANGEMENT

(11) Discrete Backprojection R^N

$(R^N g^N)(x,y) \triangleq$

$$\begin{cases} \int_0^{2\pi} \tilde{g}(\theta,\ x\cos\theta + y\sin\theta)d\theta & (11.a) \\ \int_0^{\pi} \tilde{g}(\theta,\ x\cos\theta + y\sin\theta)d\theta & (11.b) \end{cases}$$

$\tilde{g}(\theta,s)$ is a function of the continuous variable s, obtained by the interpolation of $g^N(\theta,.)$; let $\tilde{g} \triangleq I.g^N$ (I is a θ - invariant interpolation operator).

As in the continuous case, we define :

$\mathcal{L}^N_{2\pi}\ f^N \triangleq$ (11.a) $\quad \mathcal{L}^N_{\pi}\ f^N \triangleq$ (11.b)

Principal properties of $\mathcal{L}^N_{2\pi}$ and $\mathcal{L}^N_{\pi}$ are (see |6| for proof) :

P^N1- If I is a linear operator (*) (in a slightly restricted sense a convolution or a Whittaker-Shannon - Type Interpolation |7|) ; then $\mathcal{L}^N_{2\pi}$ and $\mathcal{L}^N_{\pi}$ are linear

P^N2- If $\begin{cases} \bar{f}^N(\theta,i) \triangleq \bar{f}(\theta,s_i) \\ I \text{ linear and symmetry-preserving (**)} \end{cases}$

then $\bar{f}^N(\theta,i) = f^N(\theta+\pi,-(i+1))$ (12)

and $\mathcal{L}^N_{2\pi} f^N = \mathcal{L}^N_{\pi} f^N + \mathcal{L}^N_{\pi} \bar{f}^N = \mathcal{L}^N_{\pi}(f^N + \bar{f}^N)$

P^N3- If $f^N(\theta,i) = p_\theta(s_i)$ discretization of the linear attenuation function,

then $\bar{f}^N = f^N$ and $\mathcal{L}^N_{2\pi} f^N = 2\,\mathcal{L}^N_{\pi} f^N$

(*) Do not confuse with the classical linear interpolation

(**) I is symmetry-preserving iff for any pair of discrete functions f_1^N & f_2^N which are symmetric, their images $I.f_1^N$ & $I.f_2^N$ are also symmetric.

B. Application to High Resolution

In the following, we assume that all conditions required for P^N1, P^N2 & P^N3 are fulfilled. Let Δx be the ray sampling period and $x_i = i\Delta x + \Delta x/4$ the ray sampling.
We assume also for simplicity (see Appendix 1) that the projections $p_\theta(x_i)$ are readily available.
Finally let us denote $\Delta x = 2h$ and consider the 2 sequences (s_i) and (s'_i) defined by (3) and (3').

We can write $s_{2i} = x_i$ (13)

Let's define f^N by relations (14) :

$$\begin{cases} f^N(\theta,2i) \triangleq p_\theta(x_i) & (14a) \\ f^N(\theta,2i+1) \triangleq \beta/2\ [p_\theta(x_i)+p_\theta(x_{i+1})] & (14b) \end{cases} \quad (14)$$

Using (12) & (14) we can compute $\bar{f}^N$:

$\bar{f}^N(\theta,2i) = f^N(\theta+\pi,-(2i+1)) = f^N(\theta+\pi,-2(i+1)+1)$

$= \beta/2\,[p_{\theta+\pi}(x_{-(i+1)})+p_{\theta+\pi}(x_{-i})]$

$= \beta/2\,[p_\theta(-x_{-(i+1)})+p_\theta(-x_{-i})]$

(since $p_{\theta+\pi}(y) = p_\theta(-y)$)

$\Rightarrow \bar{f}^N(\theta,2i) = \beta/2\ [p_\theta(s_{2i+1}) + p_\theta(s_{2i-1})]$ (15)

$\bar{f}^N(\theta,2i+1) = f^N(\theta+\pi, -(2i+2))$

$= \alpha\, p_{\theta+\pi}(x_{-(i+1)})$

$= \alpha\, p_\theta(-x_{-(i+1)})$

$\Rightarrow \bar{f}^N(\theta,2i+1) = \alpha\, p_\theta(s_{2i+1})$ (16)

(14a)&(15) $\Rightarrow (f^N+\bar{f}^N)(\theta,2i) = \alpha\, p_\theta(s_{2i})$

$+\beta/2\ [p_\theta(s_{2i+1})+p_\theta(s_{2i-1})]$ (17)

(14b)&(16) $\Rightarrow (f^N+\bar{f}^N)(\theta,2i+1) = \alpha\, p_\theta(s_{2i+1})$

$+\beta/2\ [p_\theta(s_{2i+2})+p_\theta(s_{2i})]$ (18)

(17)&(18) $\Rightarrow (f^N+\bar{f}^N)(\theta,i) = \alpha\, p_\theta(s_i)$

$+\beta/2\ [p_\theta(s_{i+1})+p_\theta(s_{i-1})]$ (19)

Let

$q_\theta(s) \triangleq \alpha\, p_\theta(s) + \beta/2\ [p_\theta(s+h) + p_\theta(s-h)]$ (20)

$\hat{q}_\theta \triangleq F.T\ (q_\theta)$ (F.T : Fourier Transform) (21)

$\hat{p}_\theta \triangleq F.T\ (p_\theta)$ (22)

(20),(21)et(22) $\Rightarrow \hat{q}_\theta(v) = F(v)\hat{p}_\theta(v)$

where $F(v) = \alpha + \beta\cos\pi v/v_c$ (23)

If we assume now that p_θ is band limited to $[-v_c,v_c]$; then

(23) $\Rightarrow \hat{q}_\theta = H.\hat{p}_\theta$ where

$$\left.\begin{array}{l} H(v) \triangleq F(v),\ |v| \leqslant v_c \\ H(v) \triangleq 0, \text{ else} \end{array}\right\} \quad (24)$$

if $\alpha+\beta = 1$, then H(v) is the generalized Hamming window.

(19)&(20) $\Rightarrow (f^N+\bar{f}^N)(\theta,i) = q(\theta,s_i) = q^N(\theta,i)$

$\Rightarrow \mathcal{L}^N_{2\pi} f^N = \mathcal{L}^N_{\pi}(f^N+f^N) = \mathcal{L}^N_{\pi} q^N$ (25)

Finally, let

$\hat{k} \triangleq F.T(k)$ (k kernel associated with $\mathcal{L}^N_{2\pi}$ and $\mathcal{L}^N_{\pi}$)

$k_H = F.T^{-1}(\hat{k}.H)$

$L^N_{2\pi}$ & L^N_{π} be the Reconstruction operators associated with the kernel k_H, then we obtain :

$\mathcal{L}^N_{2\pi} f^N = \mathcal{L}^N_{\pi} q^N = L^N_{\pi} p^N$ (26)

S.C. TAN, D. LE GALL, T.H. NGUYEN
M. GAMEIRO PAIS, C. BENCHIMOL

RECONSTRUCTION CONIQUE : HAUTE RESOLUTION SANS REARRANGEMENT

FAN-BEAM RECONSTRUCTION : HIGH RESOLUTION WITHOUT REARRANGEMENT

The figure below illustrates this result schematically.

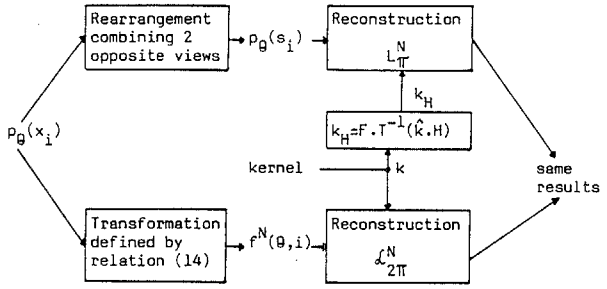

III. Fan Beam Geometry

In Fan Beam Geometry, the theory developped in section 2 is no longer exact. Actually, 2 opposite fan-projections cannot be combined as in the parallel case (see e.g |3|).

However, in the proximity of the center, the X-ray beam is nearly parallel. Therefore, the method is relevant when applied to small objects lying on or near the center. This is confirmed by simulation results. The phantom used consists of line-pairs with high spatial frequencies : 8.33, 10., 12.5, 14.33 lp/cm (fig 2). Each spatial frequency is materialized by five equally spaced lines of equal thickness.

Two machines have been simulated whose characteristics are as follow :

	M1	M2
fan angle	41°	id
number of rays	1024	2048
beam width	2x(41/1024)	id
number of views	1024	id
focal/center distance	750mm	id

DC1, DC2 are centered-phantom data computed with M1, M2 respectively. The Nyquist frequency associated to the ray sampling M1 is 10 lp/cm. Thus, the standard reconstruction with DC1 should not allow one to recover the spatial frequencies above 10 lp/cm (see fig 2a). The same data DC1, when applying the new approach to High Resolution, yield results shown in fig 2b. Fig 2c shows the results obtained with data DC2 in conjuction with the standard Reconstruction associated with the ray sampling period h = 41/2048.

As expected, there is no significant difference between fig 2b and fig 2c. Taking the 14.33 lp/cm profile in fig 2b shows clearly that spatial frequencies as high as 14.33 lp/cm are recovered (fig 2d).

We also tested the new method with the phantom lying as far away as 10 cm from the center. The gain of spatial resolution is still substantial. The effectiveness of the method has been demonstrated under conditions of real data acquisition on the THOMSON-CGR CE 10000 machine (fig 3).

IV. Conclusions

We have explored with success a new approach to High Resolution Reconstruction. This new approach presents the following advantages :

- a robustness to the mechanical imperfections (imprecision in the offset, in angular positions...) and also to patient motion. Actually, since the transformation is performed independently on each projection, the consistency of data is preserved. This is not the case with rearrangement techniques and may lead to severe artifacts |8|
- a cost-effective implementation on current 3rd generation scanners.

Comparisons of this new approach with the rearrangement techniques are under way. The results will be reported in a later publication.

Appendix 1

In reality, due to the beam width, the detector provides, instead of $p_\theta(x_i)$, values ${}^a p_\theta(x_i)$ defined as following :

$$ {}^a p_\theta(x_i) = \int_{x_i-a}^{x_i+a} p_\theta(x)dx \quad (2a = \text{beam width}) $$

Since we have also ${}^a p_{\theta+\pi}(y) = {}^a p_\theta(-y)$, every result obtained with $p_\theta(x_i)$ can be transposed simply to ${}^a p_\theta(x_i)$. In particular, we obtain :

$$ \mathcal{L}^N_{2\pi}\, {}^a f^N = \mathcal{L}^N_{\pi}\, {}^a p^N = \mathcal{L}^N_{\pi}\, p^N $$

$\mathcal{L}^N_\pi$: Reconstruction associated with the kernel ${}^a k_H$

$$ {}^a k_H(s) = \int_{s-a}^{s+a} k_H(t)dt \ ; $$

k_H : kernel associated with L^N_π.

Acknowledgements

We wish to express our since[illegible]hanks to Mrs N. Henry for typing the manuscript.

References

1. P.M. Joseph & al. : The effect of sampling on CT images in Comput. Tomogr. 4(3) : 189-206, 1980
2. R.A. Schulz & al. : A comparison of the number of rays vs. the number of views in reconstruction tomography, in Proc. Soc. Photo. Inst. Engs 127, 313-320, 1977
3. T.M. Peters & R.M. Lewitt : Computed Tomography with Fan Beam Geometry J. CAT, 1(4), 1977 - pp. 429-436
4. S.C. Tan, to be submitted for publication
5. A.C. Kak : Computerized Tomography with X-Ray, Emission, and Ultrasound Sources ; in Proc IEEE, vol. 67, n° 9, 1245-1272, Sept. 79
6. S.C. Tan, THOMSON-CGR Internal Report
7. S.W. Rowland : Image Reconstruction from Projections - implementation & applications ; ed by G.T. Herman (Springer Verlag 1979)
8. P.M. Joseph : Radiology of the skull and brain, vol 5 ; ed by T.H. Newton & G. Potts (C.V. Mosby, St-Louis, 1980)

S.C. TAN, D. LE GALL, T.H. NGUYEN
M. GAMEIRO PAIS, C. BENCHIMOL

RECONSTRUCTION CONIQUE : HAUTE RESOLUTION SANS REARRANGEMENT

FAN-BEAM RECONSTRUCTION : HIGH RESOLUTION WITHOUT REARRANGEMENT

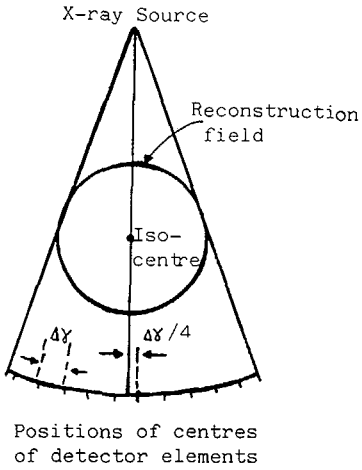

Fig 1. Fan-Beam Geometry with quarter-ray detector off-set

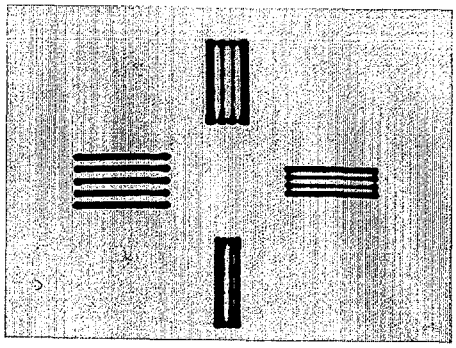

Fig 2a. Reconstruction of DC1 using standard algorithm

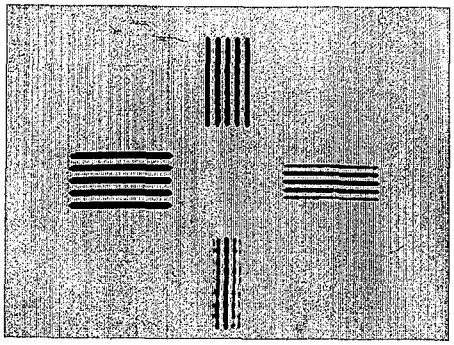

Fig 2b. Reconstruction using High Resolution algorithm

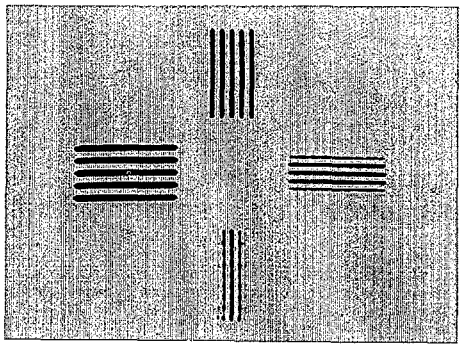

Fig 2c. Reconstruction of DC2 using standard algorithm

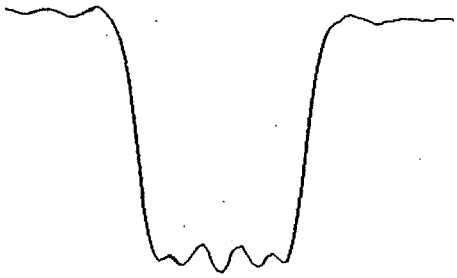

Fig 2d. Reconstruction profile of the spatial frequency 14.33 lp/cm using High Resolution algorithm

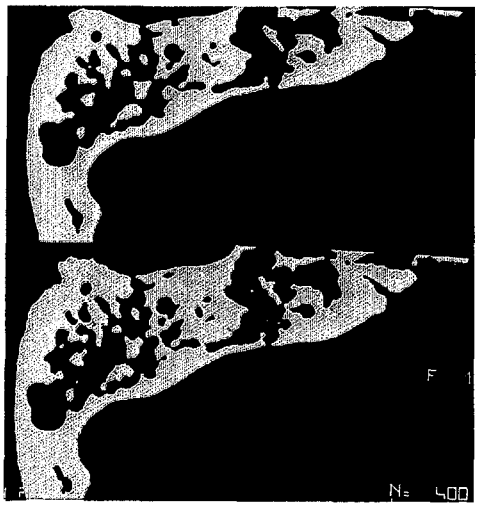

Fig 3. Reconstruction of real data acquisition (THOMSON-CGR - CE 10000 machine).(top): Standard algorithm. (bottom):High Resolution algorithm